Electroweak precision fit and new physics in light of the W boson mass

Chih-Ting Lu,[1,*] Lei Wu,[1,†] Yongcheng Wu,[1,‡] and Bin Zhu[2,§]

[1]Department of Physics and Institute of Theoretical Physics, Nanjing Normal University, Nanjing 210023, China

[2]Department of Physics, Yantai University, Yantai 264005, China

(Received 11 April 2022; accepted 3 August 2022; published 29 August 2022)

The W boson mass is one of the most important electroweak precision observables for testing the Standard Model (SM) or its extensions. The very recent measured W boson mass at the Collider Detector at Fermilab (CDF) shows about 7σ deviations from the SM prediction, which may challenge the internal consistency of the SM. By performing the global electroweak fit with the new W boson, we present the new values of the oblique parameters: $S = 0.06 \pm 0.10$, $T = 0.11 \pm 0.12$, $U = 0.13 \pm 0.09$, or $S = 0.14 \pm 0.08$, $T = 0.26 \pm 0.06$ with $U = 0$ and the corresponding correlation matrices, which strongly indicates the need for the nondegenerate multiplets beyond the SM. As a proof-of-concept, we show that the new results can be accommodated in the two-Higgs doublet model, where the charged Higgs boson has to be either heavier or lighter than both two heavy neutral Higgs bosons. The collider search for these non-SM Higgs bosons will provide a complementary way to test the new physics for W boson mass anomaly.

DOI: 10.1103/PhysRevD.106.035034

I. INTRODUCTION

The electroweak (EW) precision observables can assess the validity of the Standard Model (SM) [1] but also provide a sensitive probe of uncovering new physics beyond the SM [2,3]. Historically, the precision experiments at Large Electron-Positron (LEP) have established or supported the framework of renormalizable gauge field theories. Then, the global fit of the SM to the electroweak precision data indirectly predicted the top quark and the Higgs boson masses before their respective discoveries at the Tevareon and LHC [4]. Now, in the era of post-Higgs boson, the new particles have not been discovered at the LHC, but there exist some intriguing tensions in the precision measurements, such as the muon anomalous magnetic moment and the Cabibbo-Kobayashi-Maskawa unitarity triangle. Therefore, as history has happened, we may again observe the hints of new physics first in EW precision measurements [5–7].

In the framework of the global EW fit, the predicted W boson mass is given by [8][1]

$$m_W^{\mathrm{SM}} = 80.357 \pm 0.006\ \mathrm{GeV}, \tag{1}$$

whose precision is better than that of previous direct measurements at LEP, Tevatron, and LHC. Thus, the sensitivity of EW fit on new physics is limited by the experimental precision of m_W [6]. Therefore, improving the precision of the direct measurement of m_W is essential for the test of the SM. Very recently, with an unprecedented precision (accuracy of $\sim 1 \times 10^{-4}$), the Collider Detector at Fermilab (CDF) collaboration has reported the world's best direct measurement of the W boson mass [9],

$$m_W^{\mathrm{CDF}} = 80.4335 \pm 0.0094\ \mathrm{GeV}, \tag{2}$$

which is on the same level of precision with the EW fits and shows about 7σ deviation from Eq. (1).

The W boson mass in the SM is related with the Z-boson mass, m_Z, the fine structure constant, α, and the Fermi constant, G_μ, by

$$m_W^2\left(1 - \frac{m_W^2}{m_Z^2}\right) = \frac{\pi\alpha}{\sqrt{2}G_\mu}(1 + \Delta r). \tag{3}$$

*06285@njnu.edu.cn
†leiwu@njnu.edu.cn
‡ywu@okstate.edu
§zhubin@mail.nankai.edu.cn

[1]This quoted value appears in the review on "Electroweak Model and Constraints on New Physics" by Erler and Freitas of the Particle Data Group (PDG) volume.

Here Δr includes the quantum corrections to m_W, which depends on the top quark mass, m_t, quadratically and the Higgs mass, m_h, logarithmically. Since the relation in Eq. (3) is of central importance to the precision tests of the electroweak sector of the SM, the theoretical prediction of m_W in the SM has been calculated at the one-loop [10,11] and two-loop level [12–22], as well as leading three- and four-loop corrections [23–32]. The m_W containing all known higher-order corrections in the on-shell scheme has been given in Refs. [33,34], where the unknown higher order contributions have also been estimated to be about 4–6 MeV. Then, including these theoretical corrections, there is still about 5.1σ discrepancy from Eq. (1). This may be an underestimation of the high order corrections or systematic errors, or a hint of the new physics beyond the SM.

In this work, we first calculate the theoretical values of electroweak precision observables (EWPOs) by performing the global EW fit with the newly measured W boson mass and show the new tensions between the EW fit results and the direct measurements. Then we derive the model-independent constraints on the new physics, such as the oblique parameters S, T, and U, and discuss the implications for new physics models. Finally, we draw our conclusions.

II. ELECTROWEAK FITS

The global EW fit is a powerful tool to explore the correlations among observables in the SM and predict the direction of new physics [5,6,35–39]. Since the EW parameters in the SM are closely related to each other, we can expect some observables in the global EW fits may

TABLE I. The input parameters and the best points in the global EW fit. The Fermi constant $G_F = 1.1663787(6) \times 10^{-5}$ [GeV^{-2}] and fine-structure constant $\alpha = 1/137.035999074(44)$ [8] are fixed in our calculation. Correlations among $(m_Z, \Gamma_Z, \sigma_h^0, R_\ell^0, A_{\rm FB}^{0,\ell})$ and among $(A_{\rm FB}^{0,c}, A_{\rm FB}^{0,b}, A_c, A_b, R_c^0, R_b^0)$ are also taken into account [4]. The value of "Pull" is defined as $(O_{\rm fit} - O_{\rm measure})/\sigma$, where σ is the combined error of each input observable from fitted value and measurement.

		PDG 2021				CDF 2022				
		$\chi^2_{\rm min}({\rm dof}) = 18.74(16)$				$\chi^2_{\rm min}({\rm dof}) = 62.58(16)$				
Parameter	Input value	Fit result	Pull	Fit w/o input	Pull	Fit result	Pull	Fit w/o input	Pull	Refs
m_W [GeV]	80.379(12)	80.361(6)	−1.34	80.357(6)	−1.65	…	…	…	…	[8]
	80.4335(94)	…	…	…	…	80.380(5)	−5.00	80.357(6)	−6.83	[9]
$\Delta\alpha^{(5)}_{\rm had}$	0.02761(11)	0.02756(11)	−0.31	0.02717(38)	−2.85	0.02747(10)	−0.95	0.02609(36)	−3.99	[39–41]
m_h [GeV]	125.25(17)	125.25(17)	−0.01	$92^{(21)}_{(18)}$	−1.56	125.24(17)	−0.04	$44^{(10)}_{(8)}$	−7.96	[8]
m_t [GeV][b]	172.76(58)	173.02(56)	0.33	176.2(2.0)	1.65	173.97(55)	1.51	184.1(16)	6.47	[8]
$\alpha_s(m_Z)$	0.1179(9)	0.1180(9)	0.10	0.1193(9)	0.46	0.1177(9)	−0.17	0.1155(29)	−0.80	[8]
Γ_W [GeV]	2.085(42)	2.0905(5)	0.13	2.0905(5)	0.13	2.0918(5)	0.16	2.0918(5)	0.16	[8]
Γ_Z [GeV]	2.4952(23)	2.4942(6)	−0.43	2.4940(7)	−0.49	2.4946(6)	−0.27	2.4945(7)	−0.31	[4]
m_Z [GeV]	91.1875(21)	91.1882(21)	0.24	91.2037(90)	1.75	91.1907(20)	1.11	91.2386(79)	6.28	[4]
$A_{\rm FB}^{0,b}$	0.0992(16)	0.1031(3)	2.39	0.1033(3)	2.48	0.1035(3)	2.65	0.1037(3)	2.75	[4]
$A_{\rm FB}^{0,c}$	0.0707(35)	0.0737(3)	0.85	0.0737(3)	0.85	0.07401(25)	0.94	0.07402(25)	0.94	[4]
$A_{\rm FB}^{0,\ell}$	0.0171(10)	0.01623(10)	−0.87	0.01622(10)	−0.88	0.01636(10)	−0.74	0.01635(10)	−0.75	[4]
A_b	0.923(20)	0.93462(4)	0.58	0.93462(4)	0.58	0.93464(4)	0.58	0.93464(4)	0.58	[4]
A_c	0.670(27)	0.6679(2)	−0.08	0.6679(2)	−0.08	0.6682(2)	−0.07	0.6682(2)	−0.07	[4]
A_ℓ(SLD)	0.1513(21)	0.1471(5)	−1.95	0.1469(5)	−2.05	0.1477(5)	−1.68	0.1475(5)	−1.76	[4]
A_ℓ(LEP)	0.1465(33)	0.1471(5)	0.18	0.1469(5)	0.12	0.1477(5)	0.36	0.1475(5)	0.30	[4]
R_b^0	0.21629(66)	0.21583(10)	−0.69	0.21582(10)	−0.70	0.21580(10)	−0.73	0.21579(10)	−0.75	[4]
R_c^0	0.1721(30)	0.17222(6)	0.04	0.17222(6)	0.04	0.17223(6)	0.04	0.17223(6)	0.04	[4]
R_ℓ^0	20.767(25)	20.735(8)	−1.22	20.732(8)	−1.33	20.733(8)	−1.29	20.730(8)	−1.41	[4]
σ_h^0 [nb]	41.540(37)	41.491(8)	−1.30	41.489(8)	−1.36	41.490(8)	−1.32	41.488(8)	−1.36	[4]
$\sin^2\theta^\ell_{\rm eff}(Q_{\rm FB})$	0.2324(12)	0.23151(6)	−0.74	0.23151(6)	−0.74	0.23144(6)	−0.80	0.23143(6)	−0.80	[4]
$\sin^2\theta^\ell_{\rm eff}$(Teva)	0.23148(33)	0.23151(6)	0.10	0.23151(6)	0.10	0.23144(6)	−0.13	0.23144(6)	−0.13	[42]
$\bar{m}_c$ [GeV]	1.27(2)	1.27(2)	0.00	…	…	1.27(2)	0.00	…	…	[8]
$\bar{m}_b$ [GeV]	$4.18^{(3)}_{(2)}$	$4.18^{(3)}_{(2)}$	0.00	…	…	$4.18^{(3)}_{(2)}$	0.00	…	…	[8]

[a]Scaled with $\alpha_s(m_Z)$.
[b]0.5 GeV theoretical uncertainty is included.

suffer from new tensions once the m_W is changed. We use Gfitter [5,6,35–37] with data from Refs. [4,8,39–42] and two benchmark m_W values: (1) 80.379 ± 0.012 GeV [PDG (2021)], (2) 80.4335 ± 0.0094 GeV [CDF (2022)] to investigate the variations of these observables. The numerical results are presented in the Table I and Fig. 3.

It can be found that the PDG (2021) has $\chi^2_{\rm min}({\rm dof}) = 18.74(16)$, which is generally in good agreement with the SM predictions. However, the new CDF (2022) has $\chi^2_{\rm min}({\rm dof}) = 62.58(16)$, which means the sizable discrepancies between the best points from EW fits and input parameters, especially for m_W, m_t, m_Z, and the hadronic contribution to the shift in the fine structure constant $\Delta\alpha^{(5)}_{\rm had}$ compared with the PDG (2021) ones.

To be specific, the relation between m_W and m_Z in the $\overline{MS}$ scheme can be written as $m_W = m_Z\rho^{1/2}c_W$ where $\rho \sim 1 + \frac{3G_F m_t^2}{8\sqrt{2}\pi^2}$ and $c_W \equiv \sqrt{1-\sin^2\theta_W(m_Z)}$ is the cosine of the Weinberg angle. As shown in Table I, the global EW fits of $\sin^2\theta^{\ell}_{\rm eff}$ is consistent with the measured value, so we can only increase the m_Z and m_t to enhance the m_W. However, even the differences between the best points of m_Z and m_t are already about 2σ from the input parameters; the best points still cannot reach to the new CDF measured m_W. This explains the large and negative Pull in the second row of Table I. We also note that there was a 2.8σ discrepancy between the two most precise top quark mass measurements, 174.98 ± 0.76 GeV (DØ) [43] and 172.25 ± 0.63 GeV (CMS) [44]. While the global EW fit with the new CDF (2022) predicts the heavier top quark mass. From m_W^2 in Eq. (3), we can find the m_W^2 is anticorrelated with the fine structure constraint. Hence, the enhanced m_W value reported in CDF (2022) is related to the smaller $\Delta\alpha^{(5)}_{\rm had}$ in the EW fits. In addition, the decrease of $\Delta\alpha^{(5)}_{\rm had}$ can be translated to the smaller hadronic vacuum polarization contributions to the muon anomalous magnetic moment, $a_\mu^{\rm HVP}$ [45,46]. Therefore, the difference between $a_\mu({\rm Exp})$ and $a_\mu({\rm SM})$ can be enlarged if the $a_\mu^{\rm HVP}$ is extracted from $\Delta\alpha^{(5)}_{\rm had}$ of the global EW fits. Besides, the old tension for $A^{0,b}_{\rm FB}$ (A_l) in PDG (2021) is increased (decreased) in the EW fits with new CDF measured m_W. Hence, the measurement of $A^{0,b}_{\rm FB}$ needs special treatment in the future. On the other hand, we also show the predictions of each observable by removing its input value once a time in the EW fits in the fourth and sixth columns in the Table I. As expected, m_t, m_Z, and $\Delta\alpha^{(5)}_{\rm had}$ are sensitive to the change of m_W. Moreover, if the Higgs mass m_h measured by LHC is removed, its best point from the global EW fits is dramatically reduced. It is because the W boson mass can be written as [33]

$$m_W = m_W^0 - C_1 \ln r_h + C_2(r_t^2 - 1) - C_3 \ln r_h (r_t^2 - 1) + \cdots, \tag{4}$$

where m_W^0 is the leading order value of W boson mass, and $r_h \equiv m_h/(100\ {\rm GeV})$, $r_t \equiv m_t/(173.4\ {\rm GeV})$. C_1, C_2, and C_3 are positive coefficients. Once the m_W is increased, the prediction of m_h without its input values in the EW fits will be decreased to compensate for the difference between m_W and m_W^0. Note that without the LHC input for m_h, the CDF (2022) measurement of m_W together with other EWPOs indicates an extremely light Higgs $m_h \approx 44^{+10}_{-8}$ GeV, which is considerably inconsistent with current measurement. If the CDF (2022) measurement is confirmed by other experiments, it strongly indicates that there is unknown correction to m_W from m_h in SM or there is new physics in the scalar sector. When both m_t and m_h are not used in the EW fits, the antagonistic effect between m_t and m_h makes the allowed regions oblique. In order to fit the m_W value and minimize the total χ^2, heavier m_t and m_h are preferred as the best point. The above numerical results are visualized in Figs. 4 and 5 in the Appendix. Besides, we also use both values of m_W in PDG (2021) and CDF (2022) as the input parameters in the global EW fits, but find that the best points are just slightly different from that only using the CDF (2022).

III. NEW BOUNDS AND NEW PHYSICS

The EWPOs generically impose stringent constraints on any theory of electroweak symmetry breaking. Most of the new physics effects on precision measurements can be described by the oblique parameters S, T, and U[2] [52]. In Table II, we provide the allowed values of S, T, and U, and the correlation matrix by using the EW fit with the W mass from CDF (2022) and PDG (2021), respectively. The main differences are that the central value of U parameter predicted by CDF (2022) is much larger than that predicted by PDG (2021), and the correlations between U and S or T are mildly strengthened as well. If making $U > S, T$, one may need to introduce some new large multiplet with sufficient low masses of the components beyond the SM [53]. We note that the $\chi^2_{\rm min}$ in Table I can be reduced to 15.44 from 62.58 if including S, T, and U in the fit, which demonstrates that the oblique parameters can describe the main effects caused by newly measured W boson mass. On the other hand, since the values of U parameter are found to be very small in many new physics models, we also present the results for S and T with $\Delta U = 0$ in Table III and Fig. 1. Without the extra freedom of the U parameter, one can only increase both S and T parameters to fit m_W. It can be seen that the SM value is within the 2σ allowed region by the PDG (2021), however, which is far away from that given by CDF (2022). The overlap between the PDG (2021) and CDF (2022) results only appears in the 2σ allowed region in

[2]Besides, there are other equivalent constraints from the EWPOs, such as $(M_W, \rho, \sin^2\theta_{\rm eff})$ and $(\epsilon_1, \epsilon_2, \epsilon_3)$ parameters [47–51].

TABLE II. The values of S, T, and U and the correlation matrix allowed by the EW fit with the W boson mass from CDF (2022) and PDG (2021), respectively. $m_h = 125$ GeV and $m_t = 172.5$ GeV are used as the SM reference point.

	PDG 2021				CDF 2022			
	Result	Correlation			Result	Correlation		
13 dof	$\chi^2_{\min} = 15.42$	S	T	U	$\chi^2_{\min} = 15.44$	S	T	U
S	0.06 ± 0.10	1.00	0.90	−0.57	0.06 ± 0.10	1.00	0.90	−0.59
T	0.11 ± 0.12		1.00	−0.82	0.11 ± 0.12		1.00	−0.85
U	-0.02 ± 0.09			1.00	0.14 ± 0.09			1.00

the S-T plane. Hence, if interpreted in the new physics, the newly measured m_W by CDF may favor introducing the additional multiplets beyond the SM. With this observation, we take the two Higgs doublet model (2HDM) [54,55] as an example to show the parameter space allowed by new oblique parameters.

In the 2HDM, there are five massive spin-zero states in the spectrum $(h, H, A, H^{\pm})$ after the electroweak symmetry breaking (EWSB). As an illustration, we consider the alignment limit in which one of the two neutral CP-even Higgs mass eigenstates aligns with the direction of the scalar field vacuum expectation values (vevs) [56–61]. We assume $m_h = 125$ GeV and then the alignment limit corresponds to $\cos(\beta - \alpha) \to 0$. The new contributions to the oblique parameters in the 2HDM arise from the non-SM Higgs loops. A brief review of the 2HDM in the alignment limit and the analytic formulas of the oblique parameters S, T, and U are given in the Appendix. Note that the two-loop corrections to the ρ parameter in the 2HDM have been discussed in [62,63] and may bring some uncertainties to our results in Fig. 2. However, since these higher-order contributions are highly involved, we only consider the one-loop corrections in our study.

Given the U parameter is much smaller than the S and T parameters in our considered parameter space (c.f. Fig. 7). Thus, we use the allowed values of S and T in Table III to perform a fit by defining $\chi^2(\mathbf{O}) = (\mathbf{y} - \mu(\mathbf{O}))^T \mathbf{C}^{-1} (\mathbf{y} - \mu(\mathbf{O}))$, where $\mathbf{y}$ is the vector of central values and $\mathbf{C}$ is the covariance matrix. In Fig. 2, we show 1- and 2-σ region allowed by S and T parameters in the plane of $\Delta m_A - \Delta m_H$ using the PDG 2021 data set with the old value of m_W and the new CDF value of m_W. We find the results are symmetric about $m_H = m_A$ axis because the S and T parameters are unchanged under the exchange of m_H and m_A [c.f. Eq. (B7)]. In the fit, the T parameter is dominant because of its quadratic dependence on the masses of the new particles. However, if the mass splitting between the charged Higgs bosons and neutral Higgs bosons is too large, it will overenhance the T parameter. Besides, in general, there is a perturbative bound on the mass splittings between these scalars, e.g., $m^2_{H/A} - m^2_{H^{\pm}} \sim \bar{\lambda} v^2 < 4\pi v^2$, where v is the vev of the Higgs field and $\bar{\lambda}$ is a combination of the quartic couplings in 2HDM (c.f. (B3). Compared with the result in our PDG (2021) fit, the degenerate case $m_{H^{\pm}} = m_A = m_H$ in new CDF (2022) fit is strongly disfavored. Besides, when $m_{H^{\pm}} = m_H$ or $m_{H^{\pm}} = m_A$, T parameter vanishes because these conditions lead to an exact custodial $SU(2)$ symmetry; namely, one of the neutral scalars joins the charged scalars to form an $SU(2)$ triplet. On the other hand, if the charged Higgs mass $m_{H^{\pm}}$ lies between the masses of the two neutral scalars, m_A and m_H, the T parameter is negative. Thus, only $m_{H^{\pm}} > m_A, m_H$ or $m_{H^{\pm}} < m_A, m_H$ are allowed. However, in the former case, S parameter is inclined to be negative (c.f. Fig. 7) because of $S \sim \log(m_{H,A}/m_{H^{\pm}})$. This makes the best points lie in the latter case. Therefore, the charged

TABLE III. Same as Table II, but for S and T with $\Delta U = 0$.

	PDG 2021			CDF 2022		
$U = 0$	Result	Correlation		Result	Correlation	
14 dof	$\chi^2_{\min} = 15.48$	S	T	$\chi^2_{\min} = 17.82$	S	T
S	0.05 ± 0.08	1.00	0.92	0.15 ± 0.08	1.00	0.93
T	0.09 ± 0.07		1.00	0.26 ± 0.06		1.00

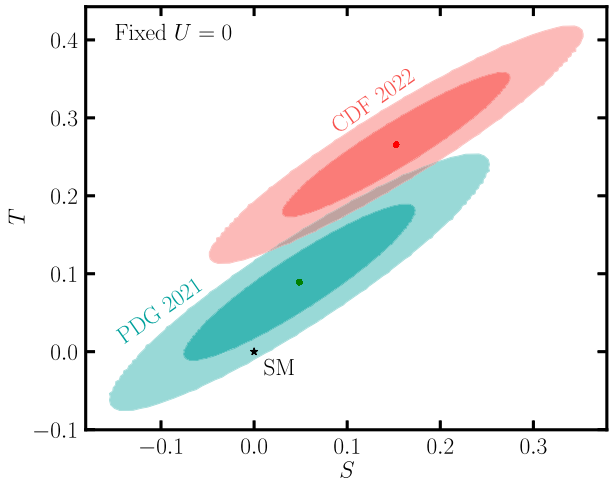

FIG. 1. The 1- and 2-σ allowed regions in S-T plane from the electroweak fits using the PDG 2021 data set with the old value of m_W (green region) and the new CDF value of m_W (red region).

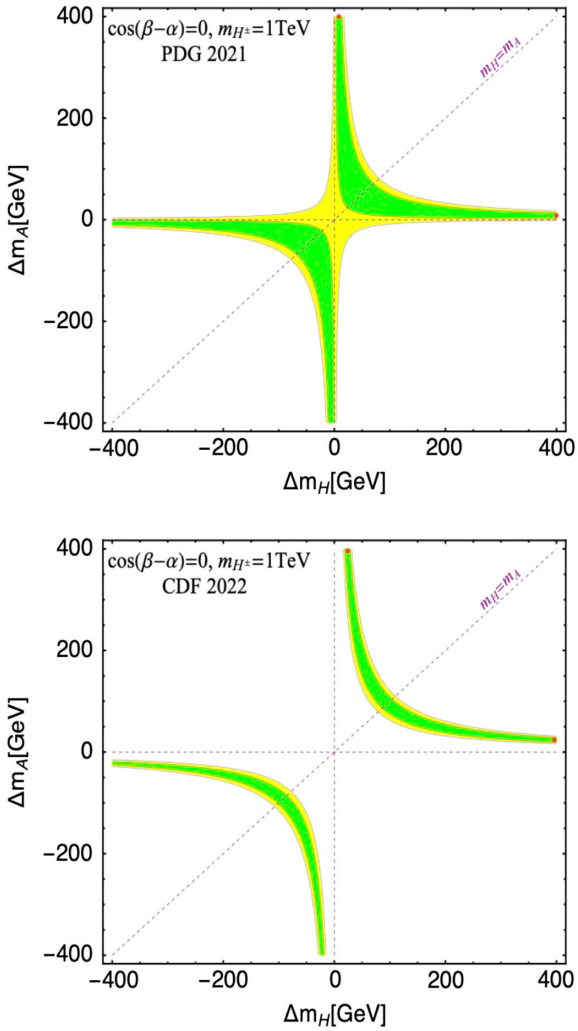

FIG. 2. The 1- and 2-σ regions allowed by the oblique parameter fit for 2HDM in the alignment limit in the plane of Δm_A versus Δm_H, where $\Delta m_A = m_A - m_{H^\pm}$ and $\Delta m_H = m_H - m_{H^\pm}$. The best points: $(\Delta m_A, \Delta m_H) = (24, 396) = (396, 24)$ GeV with $\chi^2_{\rm min} = 3.04$, $S = 0.01$ and $T = 0.173$ [CDF (2022)]; $(\Delta m_A, \Delta m_H) = (8, 400) = (400, 8)$ GeV with $\chi^2_{\rm min} = 0.24$ and $S = 0.01$, $T = 0.058$ [PDG (2021)], respectively.

Higgs boson mass $m_{H^\pm}$ has to be nondegenerate with two neutral Higgs boson masses m_A and m_H. It should be noted that there are other experimental constraints on the 2HDM (see recent examples [60,61]), such as the flavor observables, the Higgs data, and the LHC bounds. However, by performing a comprehensive global fit with the new W boson mass, the authors in Refs. [63–65] found that the parameter space for the non-SM Higgs bosons with the mass from 100 GeV to about 1 TeV in the 2HDM is still allowed, and their results are consistent with ours. Including these constraints will not change our explanation for CDF-II W boson mass measurement. In more general cases, although the Higgs doublets can mix, this will not change our main conclusion (c.f. Fig. 8). Depending on the spectrum of the heavy Higgs bosons, one may probe them in some cases at the LHC or future higher energy colliders. For example, if $H^\pm$ is the lightest new Higgs boson, it can be searched for through the process $gg \to tbH^\pm \to t\bar{t}b\bar{b}$ [66,67]. While if H or A is the lightest new Higgs boson, one can look for them through the process $gg \to t\bar{t}H/A \to t\bar{t}t\bar{t}$ [68,69]. In the regions of large $|\Delta m_A - \Delta m_H|$, the same-sign charged Higgs boson pair production provides a promising way to test our scenario [70].

IV. CONCLUSION

The very recent measurement result of m_W at CDF deviates from the SM prediction by about 7σ, which leads to deviations in the electroweak fit. Based on our analysis, we pointed out that there are new mild tensions between the predicted Z boson mass, the top quark mass, and the hadronic contribution to the shift in the fine structure constant, and the corresponding experimental measurements. Furthermore, we derived the new results of the oblique parameters S, T, and U from the electroweak fit, which strongly implies the SM extensions with new nondegenerate multiplets and their mass sequence in the spectrum. Using 2HDM as an example, we demonstrated that the charged Higgs boson, being nondegenerate with two heavy neutral Higgs bosons is required, and it has to be either heavier or lighter than both of them. The search for these non-SM Higgs bosons can be used to probe the new physics for W boson mass anomaly at the LHC and future colliders.

ACKNOWLEDGMENTS

This work is supported by the National Natural Science Foundation of China (NNSFC) under Grants No. 12147228, No. 11805161. Y. W. would like to thank U.S. Department of Energy for the financial support, under Grant No. DE-SC 0016013.

APPENDIX A: ELECTROWEAK FIT PLOTS

In Appendix A, we visualize the numerical results from Table I in Fig. 3 and also provide the one-dimensional fit results of m_t, m_Z, $\Delta\alpha^{(5)}_{had} \times 10^4$, and m_h in Fig. 4, two-dimensional fit results in $m_t - m_h$ plane in Fig. 5 and three-dimensional fit results in S-T-U space for the SM in Fig. 6. In Appendix B, we give the analytic formulas and numerical results of the oblique parameters S, T, and U in the two Higgs doublet model.

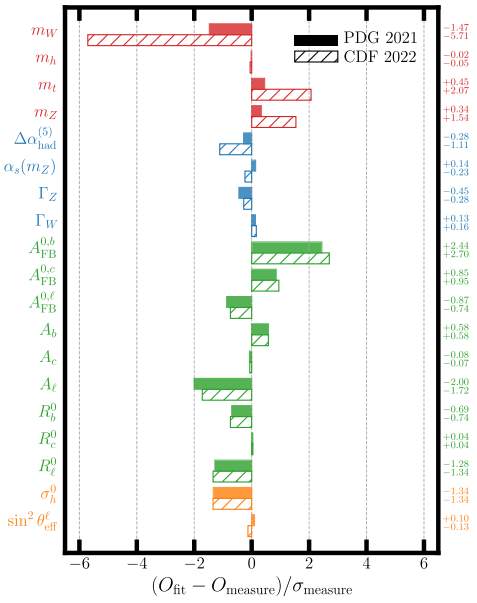

FIG. 3. The comparison of the "pull" defined in Table I between EW fits using the PDG 2021 data set with the old value of m_W and the new CDF value of m_W in the SM.

APPENDIX B: THE OBLIQUE PARAMETERS IN 2HDM

The renormalizable and CP invariant scalar potential for a general two Higgs doublet model (2HDM) with a softly broken Z_2 parity is given by

$$\begin{aligned} V(\Phi_1,\Phi_2) = {} & m_{11}^2\Phi_1^\dagger\Phi_1 + m_{22}^2\Phi_2^\dagger\Phi_2 - m_{12}^2(\Phi_1^\dagger\Phi_2 + \Phi_2^\dagger\Phi_1) \\ & + \frac{\lambda_1}{2}(\Phi_1^\dagger\Phi_1)^2 + \frac{\lambda_2}{2}(\Phi_2^\dagger\Phi_2)^2 \\ & + \lambda_3(\Phi_1^\dagger\Phi_1)(\Phi_2^\dagger\Phi_2) + \lambda_4(\Phi_1^\dagger\Phi_2)(\Phi_2^\dagger\Phi_1) \\ & + \frac{\lambda_5}{2}[(\Phi_1^\dagger\Phi_2)^2 + (\Phi_2^\dagger\Phi_1)^2], \end{aligned} \tag{B1}$$

where $\Phi_{i=1,2}$ are two scalar $SU(2)$ doublets,

$$\Phi_i = \begin{pmatrix} \phi_i^+ \\ (v_i + \phi_i^0 + iG_i^0)/\sqrt{2} \end{pmatrix}. \tag{B2}$$

After the electroweak symmetry breaking, there are five physical Higgs bosons: two charged Higgs $H^\pm$, two neutral Higgs H and h, and one neutral pseudoscalar A, whose masses are as follows:

$$\begin{aligned} m_{H^0}^2 = {} & \frac{m_{12}^2}{\sin\beta\cos\beta}\sin^2(\beta-\alpha) \\ & + v^2\left[\lambda_1\cos^2\alpha\cos^2\beta + \lambda_2\sin^2\alpha\sin^2\beta \right. \\ & \left. + \frac{\lambda_3+\lambda_4+\lambda_5}{2}\sin 2\alpha\sin 2\beta\right] \\ m_{h^0}^2 = {} & \frac{m_{12}^2}{\sin\beta\cos\beta}\cos^2(\beta-\alpha) \\ & + v^2\left[\lambda_1\sin^2\alpha\cos^2\beta + \lambda_2\cos^2\alpha\sin^2\beta \right. \\ & \left. - \frac{\lambda_3+\lambda_4+\lambda_5}{2}\sin 2\alpha\sin 2\beta\right] \\ m_{A^0}^2 = {} & \frac{m_{12}^2}{\sin\beta\cos\beta} - \lambda_5 v^2 \\ m_{H^\pm}^2 = {} & \frac{m_{12}^2}{\sin\beta\cos\beta} - \frac{\lambda_4+\lambda_5}{2}v^2. \end{aligned} \tag{B3}$$

The mixing of the neutral and charged Higgs fields is described by the angles α and β, which meet the following relations:

$$\begin{aligned} \tan\beta &= \frac{v_2}{v_1}, \\ \tan 2\alpha &= \frac{2(-m_{12}^2 + (\lambda_3+\lambda_4+\lambda_5)v_1v_2)}{m_{12}^2(v_2/v_1 - v_1/v_2) + \lambda_1 v_1^2 - \lambda_2 v_2^2}. \end{aligned} \tag{B4}$$

These two mixing angles at tree level control the couplings of the scalars with other SM particles (using Type-I as an example for Yukawa coupling):

$$g_{h^0VV} \propto \sin(\beta-\alpha) \qquad g_{H^0VV} \propto \cos(\beta-\alpha) \tag{B5}$$

$$\begin{aligned} g_{h^0ff} &\propto \frac{\cos\alpha}{\sin\beta} = \sin(\beta-\alpha) + \frac{\cos(\beta-\alpha)}{\tan\beta} \\ g_{H^0ff} &\propto \frac{\sin\alpha}{\sin\beta} = \cos(\beta-\alpha) - \frac{\sin(\beta-\alpha)}{\tan\beta}. \end{aligned} \tag{B6}$$

Under current experimental limits, the coupling of h^0 (or H^0) should be close to the SM-like Higgs boson, which can be achieved by considering the situation around *alignment* limit where $\cos(\beta-\alpha) = 0$ [or $\sin(\beta-\alpha) = 0$]. In the *alignment* limit, one of the neutral Higgs (either h^0 or H^0) is aligned with the vacuum expectation values and hence its coupling to gauge bosons tends toward the SM limit. The *alignment* limit can be easily achieved in the decoupling limit where all but the SM-like Higgs boson in the model are heavy. On the other hand, the *alignment* limit can also be attained when the other scalars are still light.

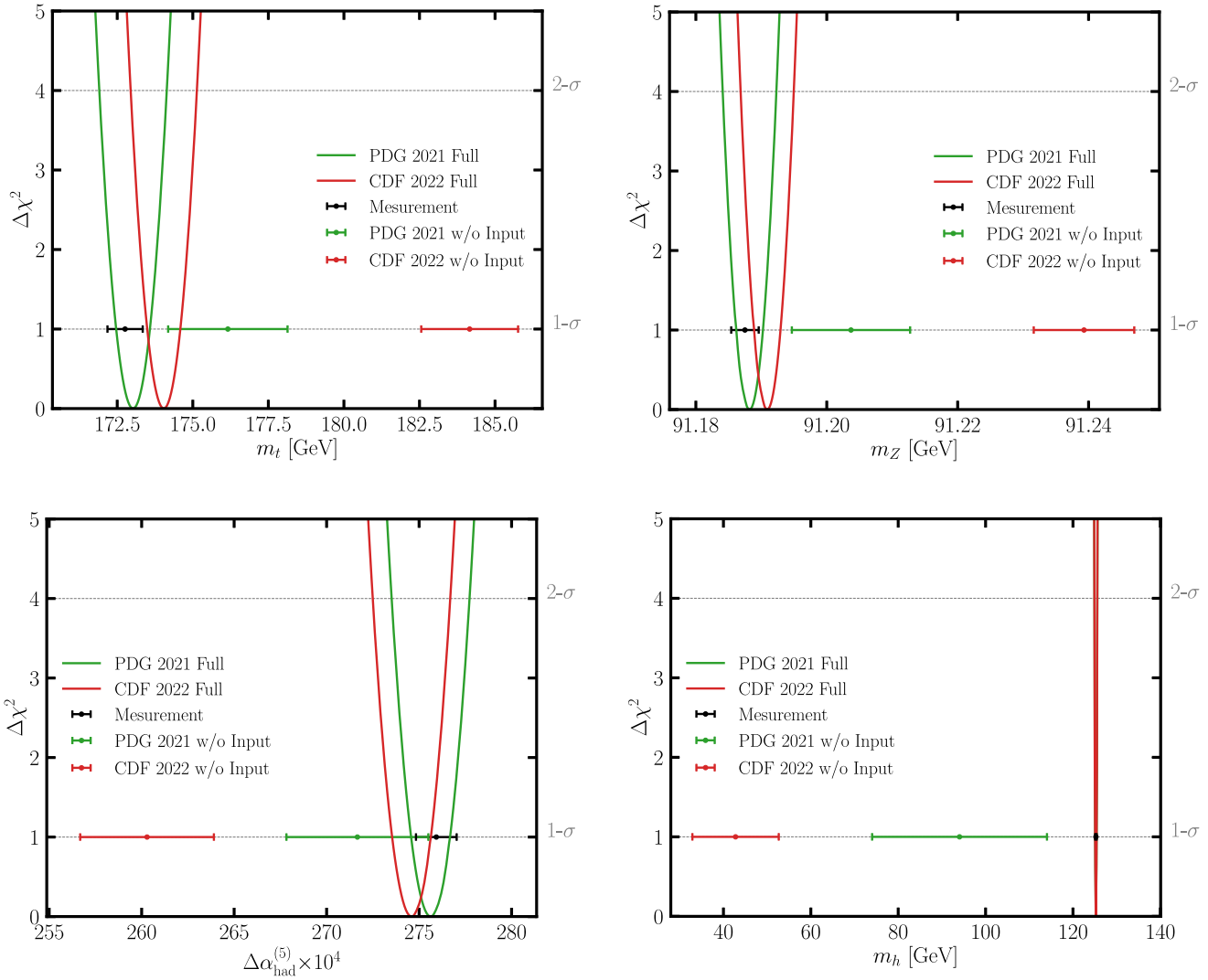

FIG. 4. Same as Fig. 3, but for 1D EW fit results in m_t, m_Z, $\Delta\alpha^{(5)}_{\rm had} \times 10^4$, and m_h.

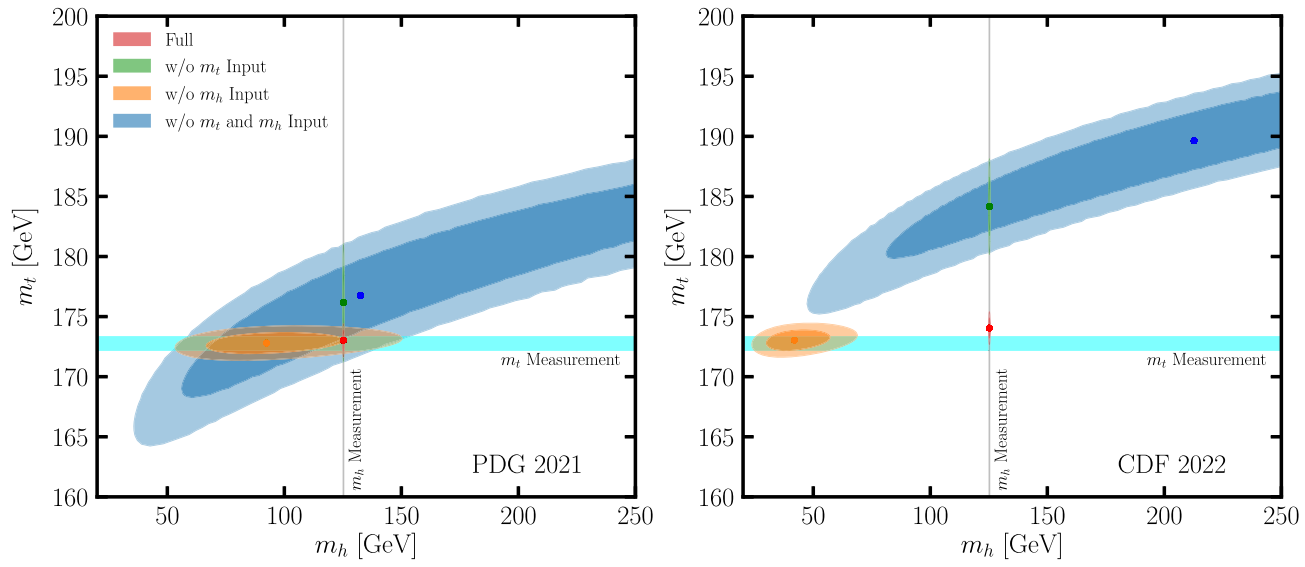

FIG. 5. Same as Fig. 3, but for 2D EW fit results in m_t-m_h plane.

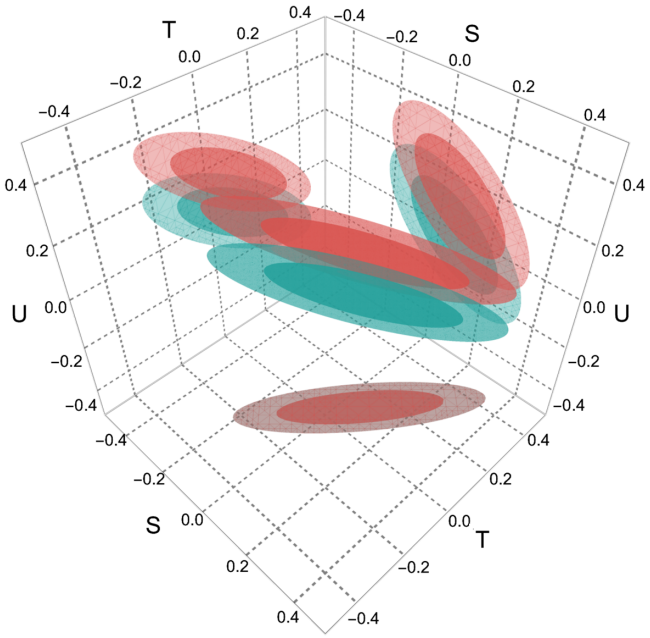

FIG. 6. Same as Fig. 3, but for 3D S/T/U fit results (old value of m_W: green region) and (new CDF value of m_W: red region) in S-T-U "space" in the SM. The projections into individual two-dimension plane are also shown.

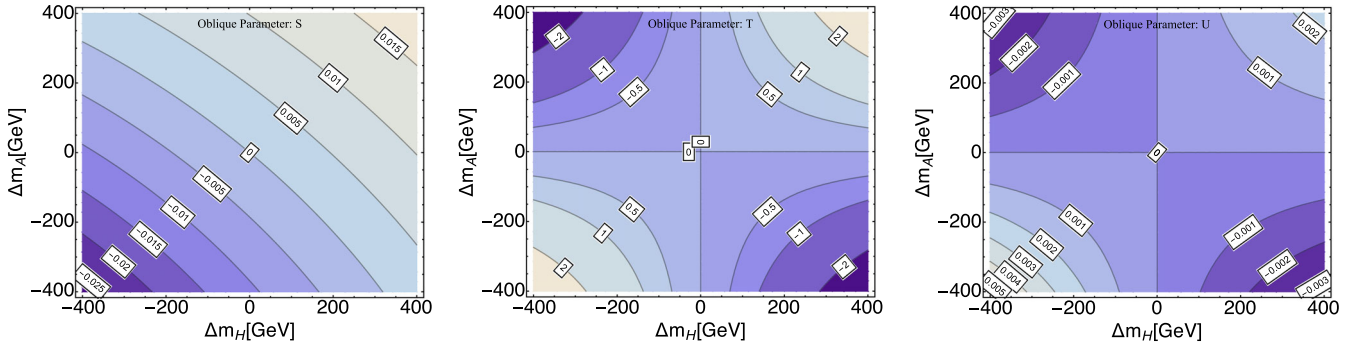

FIG. 7. Contour plots of S, T, and U for $m_{H^\pm} = 1$ TeV and $\cos(\beta - \alpha) = 0$ in Δm_H and Δm_A plane.

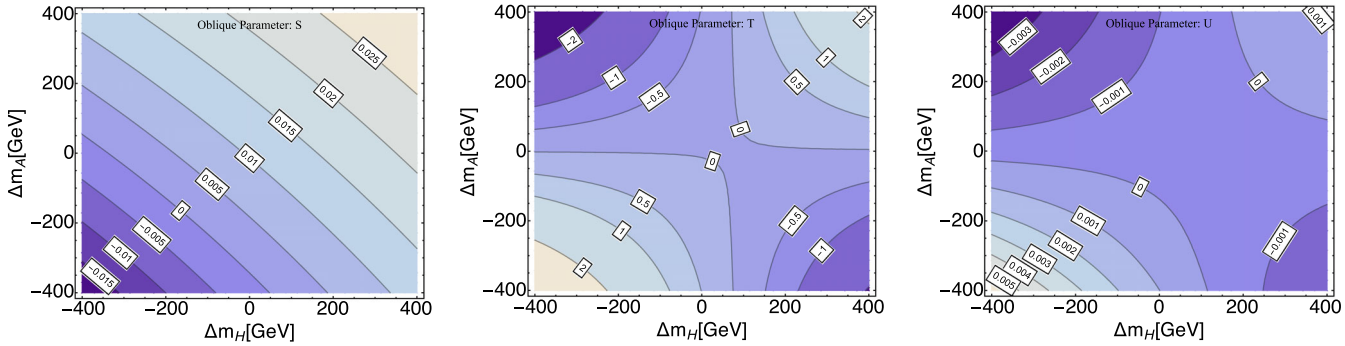

FIG. 8. Same as Fig. 7, but for $\cos(\beta - \alpha) = 0.3$.

The oblique parameters in 2HDM are given by

$$\begin{aligned}
\Delta S &= \frac{1}{\pi m_Z^2}\{[\mathcal{B}_{22}(m_Z^2;m_H^2,m_A^2)-\mathcal{B}_{22}(m_Z^2;m_{H^\pm}^2,m_{H^\pm}^2)]\\
&\quad+[\mathcal{B}_{22}(m_Z^2;m_h^2,m_A^2)-\mathcal{B}_{22}(m_Z^2;m_H^2,m_A^2)+\mathcal{B}_{22}(m_Z^2;m_Z^2,m_H^2)-\mathcal{B}_{22}(m_Z^2;m_Z^2,m_h^2)\\
&\quad-m_Z^2\mathcal{B}_0(m_Z;m_Z,m_H^2)+m_Z^2\mathcal{B}_0(m_Z;m_Z,m_h^2)]\cos^2(\beta-\alpha)\}\\
\Delta T &= \frac{1}{16\pi m_W^2 s_W^2}\{[F(m_{H^\pm}^2,m_A^2)+F(m_{H^\pm}^2,m_H^2)-F(m_A^2,m_H^2)]\\
&\quad+[F(m_{H^\pm}^2,m_h^2)-F(m_{H^\pm}^2,m_H^2)-F(m_A^2,m_h^2)+F(m_A^2,m_H^2)\\
&\quad+F(m_W^2,m_H^2)-F(m_W^2,m_h^2)-F(m_Z^2,m_H^2)+F(m_Z^2,m_h^2)\\
&\quad+4m_Z^2\bar{B}_0(m_Z^2,m_H^2,m_h^2)-4m_W^2\bar{B}_0(m_W^2,m_H^2,m_h^2)]\cos^2(\beta-\alpha)\}\\
\Delta U &= -\Delta S+\frac{1}{\pi m_W^2}\{[\mathcal{B}_{22}(m_W^2,m_A^2,m_{H^\pm}^2)-2\mathcal{B}_{22}(m_W^2,m_{H^\pm}^2,m_{H^\pm}^2)+\mathcal{B}_{22}(m_W^2,m_H^2,m_{H^\pm}^2)]\\
&\quad+[\mathcal{B}_{22}(m_W^2,m_h^2,m_{H^\pm}^2)-\mathcal{B}_{22}(m_W^2,m_H^2,m_{H^\pm}^2)+\mathcal{B}_{22}(m_W^2,m_W^2,m_H^2)-\mathcal{B}_{22}(m_W^2,m_W^2,m_h^2)\\
&\quad-m_W^2\mathcal{B}_0(m_W^2,m_W^2,m_H^2)+m_W^2\mathcal{B}_0(m_W^2,m_W^2,m_h^2)]\cos^2(\beta-\alpha)\},
\end{aligned}\tag{B7}$$

where the loop functions are provided in Ref. [71] and can be numerically calculated with LOOPTOOLS [72].

[1] W. F. L. Hollik, Fortschr. Phys. **38**, 165 (1990).
[2] P. Langacker and M.-x. Luo, Phys. Rev. D **44**, 817 (1991).
[3] P. Langacker, M.-x. Luo, and A. K. Mann, Rev. Mod. Phys. **64**, 87 (1992).
[4] S. Schael *et al.* (ALEPH, DELPHI, L3, OPAL, SLD, LEP Electroweak Working Group, SLD Electroweak Group, SLD Heavy Flavour Group Collaborations), Phys. Rep. **427**, 257 (2006).
[5] M. Baak, M. Goebel, J. Haller, A. Hoecker, D. Kennedy, R. Kogler, K. Moenig, M. Schott, and J. Stelzer, Eur. Phys. J. C **72**, 2205 (2012).
[6] M. Baak, J. Cúth, J. Haller, A. Hoecker, R. Kogler, K. Mönig, M. Schott, and J. Stelzer (Gfitter Group), Eur. Phys. J. C **74**, 3046 (2014).
[7] J. Erler and M. Schott, Prog. Part. Nucl. Phys. **106**, 68 (2019).
[8] P. A. Zyla *et al.* (Particle Data Group), Prog. Theor. Exp. Phys. **2020**, 083C01 (2020).
[9] T. Aaltonen *et al.* (CDF Collaboration), Science **376**, 170 (2022).
[10] A. Sirlin, Phys. Rev. D **22**, 971 (1980).
[11] W. J. Marciano and A. Sirlin, Phys. Rev. D **22**, 2695 (1980); **31**, 213(E) (1985).
[12] A. Djouadi and C. Verzegnassi, Phys. Lett. B **195**, 265 (1987).
[13] A. Djouadi, Nuovo Cimento A **100**, 357 (1988).
[14] B. A. Kniehl, Nucl. Phys. **B347**, 86 (1990).
[15] F. Halzen and B. A. Kniehl, Nucl. Phys. **B353**, 567 (1991).
[16] B. A. Kniehl and A. Sirlin, Nucl. Phys. **B371**, 141 (1992).
[17] A. Freitas, W. Hollik, W. Walter, and G. Weiglein, Phys. Lett. B **495**, 338 (2000); **570**, 265(E) (2003).
[18] A. Freitas, W. Hollik, W. Walter, and G. Weiglein, Nucl. Phys. **B632**, 189 (2002); **B666**, 305(E) (2003).
[19] M. Awramik and M. Czakon, Phys. Rev. Lett. **89**, 241801 (2002).
[20] M. Awramik and M. Czakon, Phys. Lett. B **568**, 48 (2003).
[21] A. Onishchenko and O. Veretin, Phys. Lett. B **551**, 111 (2003).
[22] M. Awramik, M. Czakon, A. Onishchenko, and O. Veretin, Phys. Rev. D **68**, 053004 (2003).
[23] L. Avdeev, J. Fleischer, S. Mikhailov, and O. Tarasov, Phys. Lett. B **336**, 560 (1994); **349**, 597(E) (1995).
[24] K. G. Chetyrkin, J. H. Kuhn, and M. Steinhauser, Phys. Lett. B **351**, 331 (1995).
[25] K. G. Chetyrkin, J. H. Kuhn, and M. Steinhauser, Phys. Rev. Lett. **75**, 3394 (1995).
[26] K. G. Chetyrkin, J. H. Kuhn, and M. Steinhauser, Nucl. Phys. **B482**, 213 (1996).
[27] M. Faisst, J. H. Kuhn, T. Seidensticker, and O. Veretin, Nucl. Phys. **B665**, 649 (2003).
[28] J. J. van der Bij, K. G. Chetyrkin, M. Faisst, G. Jikia, and T. Seidensticker, Phys. Lett. B **498**, 156 (2001).
[29] R. Boughezal, J. B. Tausk, and J. J. van der Bij, Nucl. Phys. **B713**, 278 (2005).
[30] R. Boughezal and M. Czakon, Nucl. Phys. **B755**, 221 (2006).
[31] K. G. Chetyrkin, M. Faisst, J. H. Kuhn, P. Maierhofer, and C. Sturm, Phys. Rev. Lett. **97**, 102003 (2006).

[32] Y. Schroder and M. Steinhauser, Phys. Lett. B **622**, 124 (2005).
[33] M. Awramik, M. Czakon, A. Freitas, and G. Weiglein, Phys. Rev. D **69**, 053006 (2004).
[34] G. Degrassi, P. Gambino, and P. P. Giardino, J. High Energy Phys. 05 (2015) 154.
[35] H. Flacher, M. Goebel, J. Haller, A. Hocker, K. Monig, and J. Stelzer, Eur. Phys. J. C **60**, 543 (2009); **71**, 1718(E) (2011).
[36] M. Baak, M. Goebel, J. Haller, A. Hoecker, D. Ludwig, K. Moenig, M. Schott, and J. Stelzer, Eur. Phys. J. C **72**, 2003 (2012).
[37] J. Haller, A. Hoecker, R. Kogler, K. Mönig, T. Peiffer, and J. Stelzer, Eur. Phys. J. C **78**, 675 (2018).
[38] J. De Blas *et al.*, Eur. Phys. J. C **80**, 456 (2020).
[39] A. Crivellin, M. Hoferichter, C. A. Manzari, and M. Montull, Phys. Rev. Lett. **125**, 091801 (2020).
[40] M. Davier, A. Hoecker, B. Malaescu, and Z. Zhang, Eur. Phys. J. C **80**, 241 (2020); **80**, 410(E) (2020).
[41] A. Keshavarzi, D. Nomura, and T. Teubner, Phys. Rev. D **101**, 014029 (2020).
[42] T. A. Aaltonen *et al.* (CDF and D0 Collaborations), Phys. Rev. D **97**, 112007 (2018).
[43] V. M. Abazov *et al.* (D0 Collaboration), Phys. Rev. Lett. **113**, 032002 (2014).
[44] A. M. Sirunyan *et al.* (CMS Collaboration), Eur. Phys. J. C **78**, 891 (2018).
[45] A. Keshavarzi, W. J. Marciano, M. Passera, and A. Sirlin, Phys. Rev. D **102**, 033002 (2020).
[46] E. de Rafael, Phys. Rev. D **102**, 056025 (2020).
[47] G. Altarelli and R. Barbieri, Phys. Lett. B **253**, 161 (1991).
[48] G. Altarelli, R. Barbieri, and S. Jadach, Nucl. Phys. **B369**, 3 (1992); **B376**, 444(E) (1992).
[49] R. Barbieri, M. Frigeni, and F. Caravaglios, Phys. Lett. B **279**, 169 (1992).
[50] G. Altarelli, R. Barbieri, and F. Caravaglios, Phys. Lett. B **314**, 357 (1993).
[51] C. P. Burgess, S. Godfrey, H. Konig, D. London, and I. Maksymyk, Phys. Rev. D **49**, 6115 (1994).
[52] M. E. Peskin and T. Takeuchi, Phys. Rev. D **46**, 381 (1992).
[53] L. Lavoura and L.-F. Li, Phys. Rev. D **49**, 1409 (1994).
[54] T. D. Lee, Phys. Rev. D **8**, 1226 (1973).
[55] G. C. Branco, P. M. Ferreira, L. Lavoura, M. N. Rebelo, M. Sher, and J. P. Silva, Phys. Rep. **516**, 1 (2012).
[56] J. F. Gunion and H. E. Haber, Phys. Rev. D **67**, 075019 (2003).
[57] N. Craig, J. Galloway, and S. Thomas, arXiv:1305.2424.
[58] M. Carena, I. Low, N. R. Shah, and C. E. M. Wagner, J. High Energy Phys. 04 (2014) 015.
[59] J. Bernon, J. F. Gunion, H. E. Haber, Y. Jiang, and S. Kraml, Phys. Rev. D **92**, 075004 (2015).
[60] N. Chen, T. Han, S. Su, W. Su, and Y. Wu, J. High Energy Phys. 03 (2019) 023.
[61] O. Eberhardt, A. P. n. Martínez, and A. Pich, J. High Energy Phys. 05 (2021) 005.
[62] S. Hessenberger and W. Hollik, Eur. Phys. J. C **77**, 178 (2017).
[63] H. Bahl, J. Braathen, and G. Weiglein, Phys. Lett. B **833**, 137295 (2022).
[64] S. Lee, K. Cheung, J. Kim, C.-T. Lu, and J. Song, arXiv: 2204.10338.
[65] H. Abouabid, A. Arhrib, R. Benbrik, M. Krab, and M. Ouchemhou, arXiv:2204.12018.
[66] G. Aad *et al.* (ATLAS Collaboration), J. High Energy Phys. 06 (2021) 145.
[67] A. M. Sirunyan *et al.* (CMS Collaboration), J. High Energy Phys. 07 (2020) 126.
[68] ATLAS Collaboration, Technical Report No. ATLAS-CONF-2022-008, CERN, Geneva, 2022, https://cds.cern.ch/record/2805212.
[69] A. M. Sirunyan *et al.* (CMS Collaboration), Eur. Phys. J. C **80**, 75 (2020).
[70] M. Aiko, S. Kanemura, and K. Mawatari, Phys. Lett. B **797**, 134854 (2019).
[71] G. 't Hooft and M. J. G. Veltman, Nucl. Phys. **B153**, 365 (1979).
[72] T. Hahn and M. Perez-Victoria, Comput. Phys. Commun. **118**, 153 (1999).